



## $\Lambda_b$ Lifetime Using $1 fb^{-1}$ Data Taken With Two Displaced Track Triggers

Text for the blessed web page – CDF note 9408 v2.0

The CDF Collaboration  
URL <http://www-cdf.fnal.gov>  
(Dated: April 22, 2009)

We report a measurement of the lifetime of the  $\Lambda_b^0$  baryon in  $p\bar{p}$  collisions at  $\sqrt{s} = 1.96$  TeV. Analyzing  $1070 \pm 60 \text{ pb}^{-1}$  of data taken using the CDF two displaced track triggered dataset we have obtained a clean sample of  $\sim 3,000$  fully reconstructed  $\Lambda_b^0 \rightarrow \Lambda_c^+ \pi^-$  decays (with  $\Lambda_c^+$  subsequently decaying via  $\Lambda_c^+ \rightarrow p^+ K^- \pi^+$ ). We fit this sample for the lifetime of the  $\Lambda_b^0$  baryon, and find;

$$c\tau(\Lambda_b^0) = 420.1 \pm 13.7 \text{ (stat)} \pm 10.6 \text{ (syst)} \mu\text{m}.$$

## I. INTRODUCTION

The lifetime of  $\Lambda_b^0$  baryons is a topic of considerable recent interest. In a simple quark spectator model, where the  $b$ -quark is approximated by a static object decaying with no interaction with the neighboring light degrees of freedom the lifetimes of all  $B$  hadrons are expected to be the same. However, because of significant non-spectator effects, the  $B$  hadron lifetimes follow a hierarchy;  $\tau(B^+) \geq \tau(B^0) \sim \tau(\Lambda_b^0) > \tau(\Lambda_c^0) \gg \tau(B_c^+)$ . This hierarchy is predicted by the Heavy Quark Expansion (HQE) technique [1], which expresses decay widths of heavy hadrons as an expansion in inverse powers of the heavy quark mass (*i.e.*  $1/m_b$ ). In the second order of this expansion, Fermi motion of the  $b$ -quark and its spin interaction with the light quark pair in  $\Lambda_b^0$  result in a shorter  $\Lambda_b^0$  lifetime compared to the  $B$  mesons. In the third order of  $1/m_b$ , non-spectator effects modify the baryon and meson lifetimes differently and lead to their hierarchy.

The ratio  $\tau(\Lambda_b^0)/\tau(B^0)$  has been the source of theoretical scrutiny since earlier calculations predicted a value larger than 0.90, almost  $2\text{-}\sigma$  above the world average at that time. These predictions cluster around a most likely central value of 0.94[2]. Equation 1 lists the results of a recent calculation[3] of  $B$  hadron lifetime ratios.

$$\begin{aligned}\tau(B^+)/\tau(B^0) &= 1.06 \pm 0.02, \\ \tau(B_s^0)/\tau(B^0) &= 1.00 \pm 0.01, \\ \tau(\Lambda_b^0)/\tau(B^0) &= 0.88 \pm 0.05.\end{aligned}\tag{1}$$

The results listed in Equation 1 reflect a HQE calculation up to  $O(1/m_b^4)$  which reduces the disagreement with the PDG  $\tau(\Lambda_b^0)/\tau(B^0)$  world average of  $0.804 \pm 0.049$ [4].

More recently CDF has reported two measurements of  $\Lambda_b^0$  lifetime in the  $\Lambda_b^0 \rightarrow J/\psi \Lambda$  channel, that differ by  $\sim 2\sigma$  from the world average [5]. In contrast with earlier discrepancy, these measurements are significantly higher than the HQE prediction. Figure I summarizes several measurements of  $\Lambda_b^0$  lifetime as well as the world average.

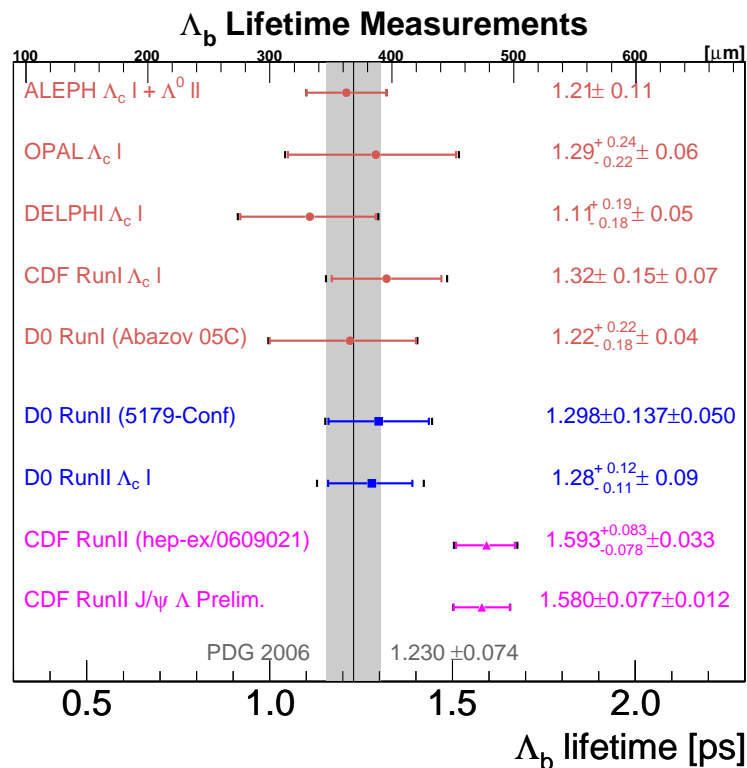


FIG. 1: A summary of recent  $\Lambda_b^0$  measurements compared to the 2006 world average. Recent CDF measurements suggest a longer  $\Lambda_b^0$  lifetime than has previously been measured.

Using a clean and high statistics sample of fully reconstructed  $\Lambda_b^0 \rightarrow \Lambda_c^+ \pi^-$  decays, this analysis hopes to shed light on the long standing discrepancy between the world average of  $\Lambda_b^0$  lifetime and its HQE prediction. A sample of  $\sim 3,000$   $\Lambda_b^0 \rightarrow \Lambda_c^+ \pi^-$  decays are reconstructed from  $1070 \pm 60$   $pb^{-1}$  of data, collected using the CDF Two displaced Track Trigger (TTT). Because

of the track displacement requirement at the trigger, the lifetime distribution is biased. We correct for the bias by employing a Monte Carlo based approach, already applied successfully to other CDF lifetime analyses [6].

## II. ANALYSIS STRATEGY

In a detector with a perfect resolution and without a trigger bias, the distribution of the proper decay length,  $ct'$  of an unstable particle with true lifetime,  $\tau$ , follows a simple exponential distribution, given by the probability density function (PDF)

$$P(ct') = \frac{1}{c\tau} e^{-\frac{ct'}{c\tau}}. \quad (2)$$

In a real detector, each measurement of  $ct'$  has an uncertainty  $\sigma_{ct}$  associated with it. This smearing of the true  $ct'$  which results in the measured value  $ct$  is accounted for by convolving the measured lifetime with a function to describe the detector resolution. The resolution function,  $R(ct, \sigma_{ct}; ct')$ , is the PDF of the measured  $ct$  and  $\sigma_{ct}$  given the true value of  $ct'$ . With this addition, the PDF for the measured proper decay length distribution becomes

$$P(ct|\sigma_{ct}) = \frac{1}{c\tau} e^{-\frac{ct'}{c\tau}} \otimes R(ct, \sigma_{ct}; ct'). \quad (3)$$

The PDF  $P(ct|\sigma_{ct})$ , is a one-dimensional conditional PDF that predicts the probability of observing this value of  $ct$  given the value of  $\sigma_{ct}$ . In order to obtain a proper two-dimensional PDF for both  $ct$  and  $\sigma_{ct}$  based on the conditional probability, the  $\sigma_{ct}$  distribution (PDF) must multiply  $P(ct|\sigma_{ct})$ . So the full two-dimensional  $ct$ - $\sigma_{ct}$  PDF becomes;

$$\begin{aligned} P(ct, \sigma_{ct}) &= P(ct|\sigma_{ct}) \cdot P(\sigma_{ct}) \\ &= \frac{1}{c\tau} e^{-\frac{ct'}{c\tau}} \otimes R(ct, \sigma_{ct}; ct') \cdot P(\sigma_{ct}) \end{aligned} \quad (4)$$

where  $P(\sigma_{ct})$  is the distribution of  $\sigma_{ct}$  observed in data. Figure 2 shows the signal and background  $\sigma_{ct}$  distributions obtained from the  $\Lambda_b^0$  signal and upper sideband regions, respectively.

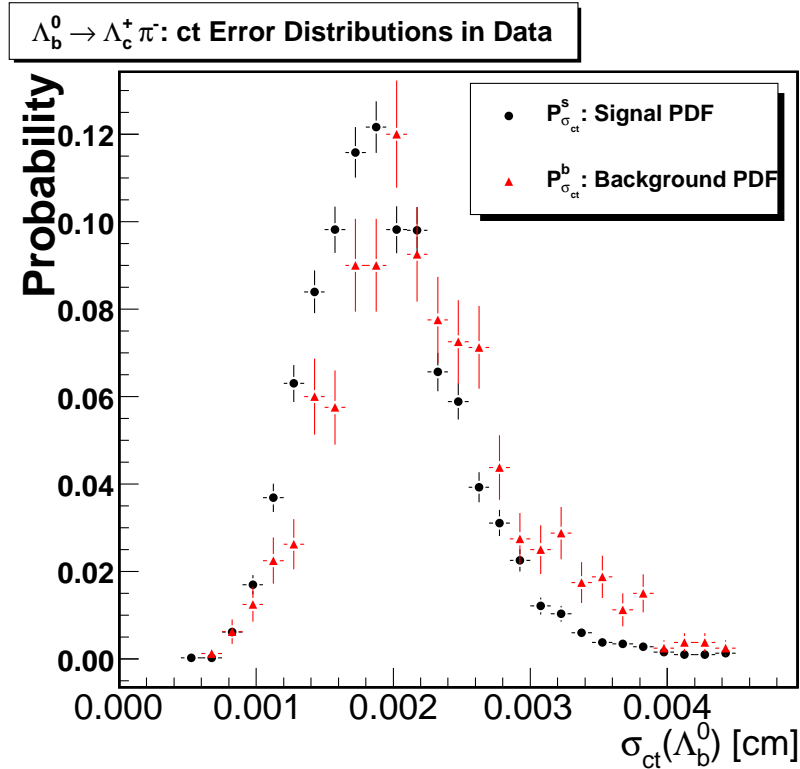


FIG. 2: The  $\Lambda_b^0$   $\sigma_{ct}$  distributions in data.

The value of  $\sigma_{ct}$ , obtained by a vertex-constrained kinematic fit is usually underestimated due to lack of knowledge of detector hit resolutions and track parameter errors due to wrong hit assignment. To account for these effects,  $\sigma_{ct}$  estimated by a vertex fit is multiplied by a scale factor  $S_{ct}$ . We estimate this scale factor by comparing the true  $ct'$  obtained from the MC truth information in the  $\Lambda_b^0 \rightarrow \Lambda_c^+ \pi^-$  signal Monte Carlo with the  $ct$  measured in the same event. A double-Gaussian resolution model is preferred by our data:

$$R(ct, \sigma_{ct}) = f \cdot \text{Gauss}(S_1 \cdot \sigma_{ct}) + (1 - f) \cdot \text{Gauss}(S_2 \cdot \sigma_{ct});$$

Where the relative fraction,  $f = 0.76$ , and the scale factor widths,  $S_1 = 1.107$  and  $S_2 = 1.508$ . Throughout this analysis, the same fraction and relative widths are used to model the resolution. In particular, when generating the trigger (SVT) efficiency and fitting the signal Monte Carlo sample.

When fitting data, it is impossible to measure the  $ct$  resolution directly as done for the Monte Carlo. A global scale factor,  $S_{ct}^{data}$ , is used instead to scale  $\sigma_{ct}$ . The value of the narrow Gaussian is set to  $S_{ct}^{data}$  while the broad Gaussian is scaled in order to maintain the same relative widths between  $S_1$  and  $S_2$  as measured in the Monte Carlo. The choice of  $S_{ct}^{data}$  is somewhat arbitrary and is treated as a source of systematic error.

In addition to the detector resolution, the Two Track Trigger (TTT) introduces a bias on the observed proper decay length. The TTT selects events with two displaced tracks which removes both the events with the short proper decay lengths, and those with very long ones. The resulting distribution is not an exponential any more, and this significantly complicates the extraction of the lifetime. An efficiency function,  $\epsilon_{TTT}(ct)$ , is introduced to parameterize the trigger and offline selection effects and is computed using  $\Lambda_b^0 \rightarrow \Lambda_c^+ \pi^-$  signal Monte Carlo.

With the addition of the  $\sigma_{ct}$  scale factor  $S_{ct}$  and the efficiency function,  $\epsilon_{TTT}(ct)$ , the joint two-dimensional  $ct - \sigma_{ct}$  PDF becomes

$$P(ct, \sigma_{ct}; S_{ct}) = P(ct | \sigma_{ct}, S_{ct}) \cdot P(\sigma_{ct}) \cdot \epsilon_{TTT}(ct). \quad (5)$$

A sample of pure signal Monte Carlo events are used to model the effect of the trigger and analysis cuts on measuring the lifetime. The efficiency function is of the form;

$$\epsilon_{TTT}(ct) = \frac{\text{Histo}_{smoothed}^{TTT}(ct)}{\sum_i \exp(ct^i, c\tau^{MC}) \otimes R(ct^i, \sigma_{ct}^i)}. \quad (6)$$

The numerator is a smoothed histogram of the proper decay length for all Monte Carlo events that pass the trigger and analysis selection criteria. The denominator is the resolution-smear lifetime, calculated analytically at every numerator bin and summed over all events (indexed by  $i$ ) that pass the cuts required to fill the numerator. Figure 3 shows the resulting TTT efficiency histogram.

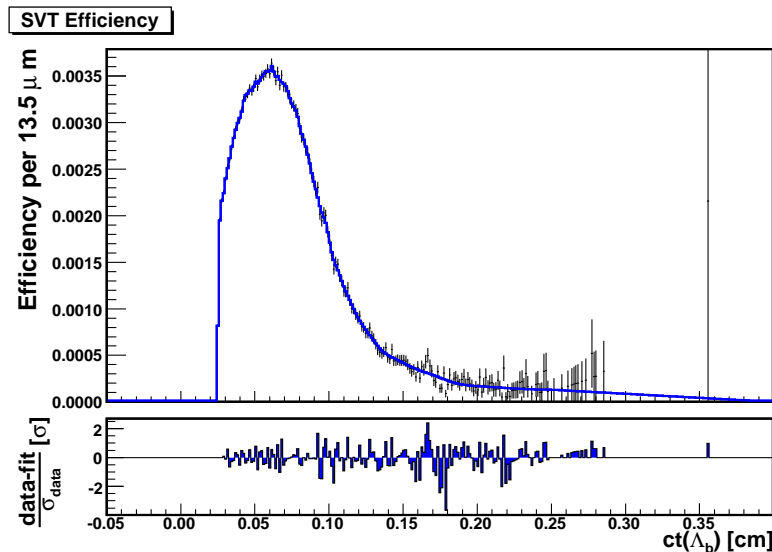


FIG. 3: The  $\Lambda_b^0$  TTT efficiency distribution.

To obtain the lifetime of the  $\Lambda_b^0$  baryon, we first determine the sample composition using a binned maximum likelihood fit of the invariant mass distribution of the  $\Lambda_c^+ \pi^-$  candidates. Second, the sample composition is fixed and an un-binned maximum-likelihood fit in  $ct$  and  $\sigma_{ct}$  is executed for the  $\Lambda_b^0$  lifetime. In the second step, only events in the  $\Lambda_b^0$  signal region are fit. The

mass PDFs are integrated over the signal mass region, and multiplied by the corresponding normalizations to obtain the sample composition of the *signal* region. This yields  $N_{\text{sig}}^i$ , the number of events of each component in the signal region.

The likelihood of one event is a sum over several fit components,  $j$ , of two-dimensional distribution functions;

$$\mathcal{L}(ct, \sigma_{ct}) = \sum_j N_{\text{sig}}^j \cdot P_{ct}^j(ct|\sigma_{ct}) \cdot P_{\sigma_{ct}}^j(\sigma_{ct}). \quad (7)$$

Here  $P_{ct}^j$  is the probability distribution of  $ct$  – a product of the proper time of the  $\Lambda_b^0$  decay,  $t$ , and the speed of light  $c$ .  $P_{\sigma_{ct}}^j$  is the probability distribution of the error on  $ct$ . In this fit, all values of  $N_{\text{sig}}^j$  are fixed, and the  $\Lambda_b^0$  lifetime is the sole parameter allowed to float. Moreover, several of the background components do not contribute to the signal region and are ignored in the lifetime fit. All the procedures were established without a knowledge of the  $\Lambda_b^0$  lifetime to be measured from the data.

### III. DATA SAMPLES

We analyze events collected by the CDF detector from February 2002 through February 2006, with an integrated luminosity of  $\mathcal{L} = 1070 \pm 60 \text{ pb}^{-1}$ , using CDF two displaced track trigger. We reconstruct a  $\Lambda_b^0$  candidate via its decay to a  $\Lambda_c^+$  and a pion, where  $\Lambda_c^+$  further decays to a proton, kaon and a pion. A  $\Lambda_c^+$  candidate is first reconstructed by requiring three tracks, with respectively proton, kaon and pion hypotheses, to have sufficient hits in tracking detectors and each track must have an impact parameter ( $d_0$ ) from the primary vertex of less than 0.1 cm and a transverse momentum of more than 500 MeV/c. The proton candidate is additionally required to have a transverse momentum greater than the pion candidate, and greater than 2.0 GeV/c. A successful  $\Lambda_c^+$  candidate is required to satisfy the following cuts after a kinematic fit of the three tracks to a common vertex:

- $\chi_{xy}^2 < 30$
- $p_T(\Lambda_c^+) > 4.3 \text{ GeV}/c$
- $2.269 < |M(pK\pi)| < 2.301 \text{ GeV}/c^2$ .

The  $\Lambda_c^+$  candidate is then paired with a pion which passes track quality cuts, an impact parameter  $< 0.1$  cm and a transverse momentum ( $p_T$ ) of  $> 2.0 \text{ GeV}/c$ . A successful  $\Lambda_b^0$  candidate is required to satisfy the following cuts after a kinematic fit of the  $\Lambda_c^+$  and pion candidates to common vertex, where the mass of the  $pK\pi$  candidate is constrained to the  $\Lambda_c^+$  mass from the PDG [4]:

- $\chi_{xy}^2 < 30$
- $4.8 < |M(pK\pi\pi)| < 7.0 \text{ GeV}/c^2$
- $p_T(pK\pi\pi) > 6.0 \text{ GeV}/c$
- $-0.007 < ct(\Lambda_c^+) < 0.028 \text{ cm}$  (w.r.t to  $\Lambda_b^0$  vertex)
- $ct(\Lambda_b^0) > 0.025 \text{ cm}$ .

These are the basic requirements to reconstruct a  $\Lambda_b^0$  candidate from the data sample. Table I lists a set of optimized cuts and Table II lists the cuts for offline confirmation of the two displaced track trigger, which are subsequently applied to the  $\Lambda_b^0$  candidate to obtain the final sample for our analysis. Using these cuts we obtain a  $\Lambda_b^0 \rightarrow \Lambda_c^+ \pi^-$  yield of  $2927 \pm 58$  candidates in the signal region  $m(\Lambda_b^0) \in [5.565, 5.670] \text{ GeV}/c^2$ , with the  $\Lambda_b^0$  mass plot shown in Figure 4.

As explained earlier, the two track trigger (TTT) efficiency,  $\epsilon_{TTT}(ct)$ , is obtained from the Monte Carlo simulation. In order to ensure that this procedure is not influenced by fluctuations, the Monte Carlo sample of  $\Lambda_b^0 \rightarrow \Lambda_c^+ \pi^-$  decays from which  $\epsilon_{TTT}(ct)$  is derived needs to be very large. A signal sample was produced using the CDF HeavyQuarkGenerator (HQGen) package, which directly produces  $B$ -hadrons following a known kinematic distribution measured from the data. The resulting  $\Lambda_b^0$  hadrons are decayed to the signal decay mode using the EvtGen package using  $c\tau^{MC}(\Lambda_b^0) = 368.0 \mu\text{m}$ . The events are then subjected to the realistic simulations of the CDF detector which uses a charge deposition model tuned on data, and includes dead channels and noisy channels. Including the dead regions from the SVXII detector is important, since the Silicon Vertex Trigger (SVT) track reconstruction algorithm requires hits on four out of five SVXII layers, and thus the position of dead SVX chips and ladders influences the SVT efficiency. The tracking detector data are then input into the trigger emulators, producing decisions bitwise identical to the algorithms implemented in the firmware of the trigger systems. It is important that the SVT behavior be modeled

Variable	Cut value
	B_CHARM_SCENA
$p_T(\pi_b^-)$	$> 2 \text{ GeV}/c$
$p_T(p)$	$> 2 \text{ GeV}/c$
$p_T(p)$	$> p_T(\pi^+)$
$p_T(K^-)$	$> 0.5 \text{ GeV}/c$
$p_T(\pi^+)$	$> 0.5 \text{ GeV}/c$
$ct(\Lambda_b^0)$	$> 250 \mu\text{m}$
$ct(\Lambda_b^0)/\sigma_{ct}$	$> 10$
$ d_0(\Lambda_b^0) $	$< 80 \mu\text{m}$
$ct(\Lambda_c^+ \leftarrow \Lambda_b^0)$	$> -70 \mu\text{m}$
$ct(\Lambda_c^+ \leftarrow \Lambda_b^0)$	$< 200 \mu\text{m}$
$ m(pK^- \pi^+) - m(\Lambda_c^+)_{PDG} $	$< 16 \text{ MeV}/c^2$
$p_T(\Lambda_b^0)$	$> 6.0 \text{ GeV}/c$
$p_T(\Lambda_c^+)$	$> 4.5 \text{ GeV}/c$
$\text{Prob}(\chi^2_{3D})$ of $\Lambda_b^0$ vertex fit	$> 0.1\%$

TABLE I: Analysis cuts determined for  $\Lambda_b$  reconstruction.

Quantity	Cut value
$Q(trk1) \times Q(trk2)$	$< 0$
$p_T(trk1) + p_T(trk2)$	$> 5.5 \text{ GeV}/c$
$p_T(trk1)$	$> 2.0 \text{ GeV}/c$
$p_T(trk2)$	$> 2.0 \text{ GeV}/c$
$ z_0(trk1) - z_0(trk2) $	$< 5.0 \text{ cm}$
$ D0_{SVT}(trk1) $	$[0.012, 0.1] \text{ cm}$
$ D0_{SVT}(trk2) $	$[0.012, 0.1] \text{ cm}$
$p_T(SVT)(trk1)$	$> 2.0 \text{ GeV}/c$
$p_T(SVT)(trk2)$	$> 2.0 \text{ GeV}/c$
$\Delta\phi(trk1, trk2)$	$[2^\circ, 90^\circ]$

TABLE II: Cuts used for offline confirmation of the two displaced track trigger

as accurately as possible, since the SVT tracks in the Monte Carlo simulation are the basis for the TTT efficiency which is the crux of this measurement.

After simulating the detector sculpting by SVT, the events are reconstructed using the standard production executable. The decay  $\Lambda_b^0 \rightarrow \Lambda_c^+ \pi^-$  is reconstructed from this sample using the same analysis cuts and trigger confirmation as the data. To mimic in Monte Carlo the run conditions and calibrations in the data, our Monte Carlo employs luminosity weighted run lists matched to data. After the trigger and offline reconstruction selection cuts, there are approximately *one million* events.

Kinematic agreement between Monte Carlo and data is critical to correctly measuring the lifetime of  $\Lambda_b^0$ . We re-weight Monte Carlo in the  $\Lambda_c^+$  Dalitz fractions,  $\Lambda_b^0$  polarization, pairs of stable tracks that satisfy the TTT requirements, and  $p_T(\Lambda_b^0)$  to match the distributions observed in the data. After re-weighting, a sample of about 270,000 signal Monte Carlo events remain. Figure 5 compares data and re-weighted Monte Carlo distributions of track pairs that satisfy TTT requirements.

#### IV. RESULTS

Based on the result of the  $\Lambda_b^0$  mass fit (shown in Figure 4), we define our signal region to be  $5.565 < m(\Lambda_c^+ \pi^-) < 5.67 \text{ GeV}/c^2$  with normalizations listed in Table III. Only the signal region is used when fitting for the lifetime. In some lifetime fits, the upper sideband is included explicitly, and the parametric shape of the combinatorial background is allowed to float in a combined signal plus sideband region fit. We chose not to follow this approach in favor of a less complicated, faster fit. We have studied changes to the shape of the combinatorial background along the  $ct$  axis. Since the ratio of the  $\Lambda_b^0$  signal to combinatorial background in the signal region is about 30 : 1, the shape of the combinatorial background lifetime has sub-micron influence on the final lifetime fit (*i.e.*, on the order of 0.2 – 0.3  $\mu\text{m}$ ), and is therefore negligible.

The result of the un-binned, maximum likelihood,  $\Lambda_b^0$  lifetime fit on data is

$$c\tau(\Lambda_b^0) = 420.1 \pm 13.7 \mu\text{m} \quad (8)$$

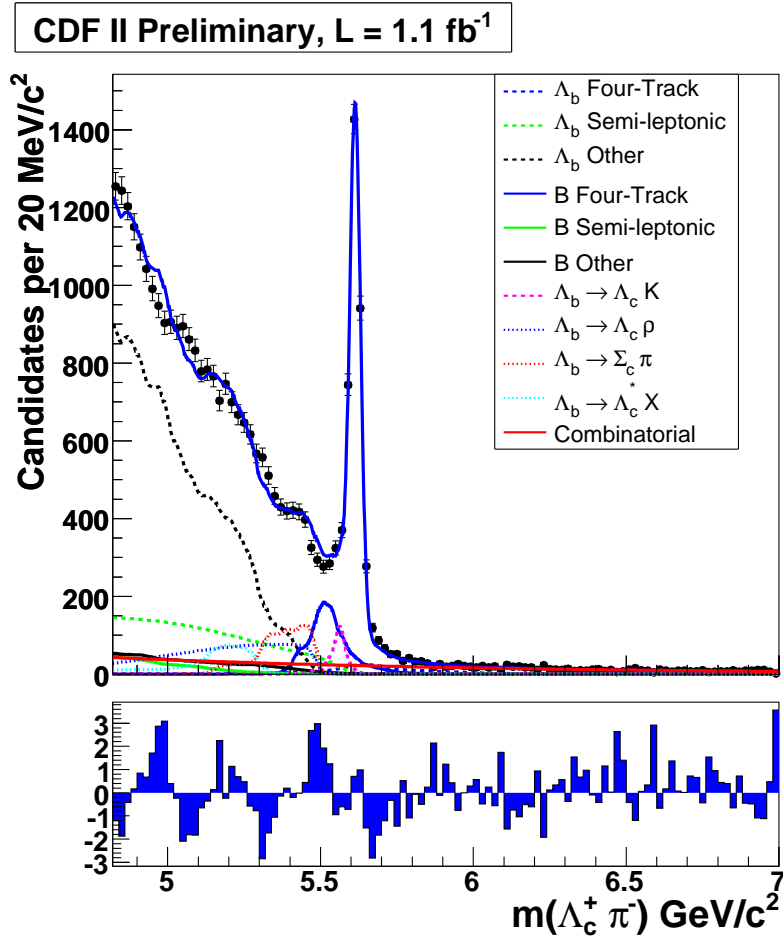


FIG. 4:  $\Lambda_b^0$  mass fit. The solid blue line is the total fit. The primary background components are listed in the legend.

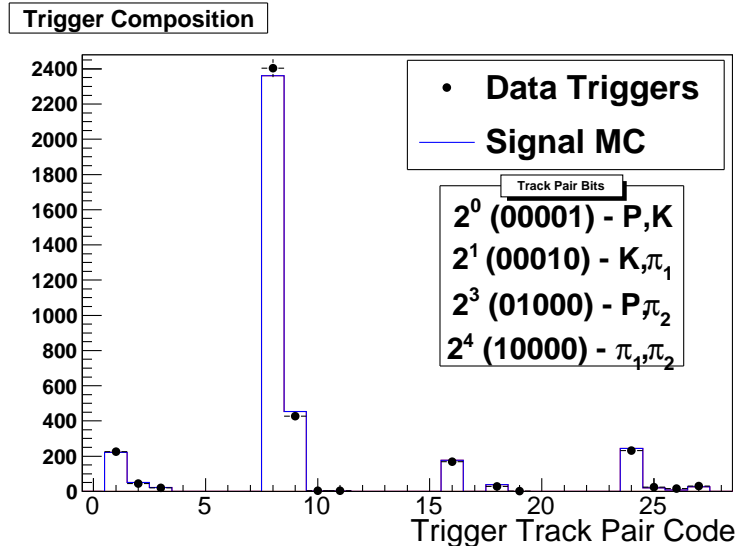


FIG. 5: Comparison of data and re-weighted Monte Carlo distributions of track pairs that satisfy TTT requirements.

The resulting likelihood projected onto the  $ct$ -axis is shown in Figure 6. The fit probability is estimated to be 37% using an unbinned Kolmogorov-Smirnov test.

Normalization	Value
$N_{\Lambda_b^0 \rightarrow \Lambda_c^+ \pi^-}$	$2904.9 \pm 57.9$ (82%)
$N_{B \text{ Four-Track}}$	$250.5 \pm 15.4$ (7%)
$N_{\Lambda_b^0 \rightarrow \Lambda_c^+ K^-}$	$138.6 \pm 15.9$ (4%)
$N_{\text{Combinatorial}}$	$116.2 \pm 5.0$ (3%)
$N_{\Lambda_b^0 \text{ Four-Track}}$	$113.7 \pm 15.9$ (3%)
$N_{\Lambda_b^0 \rightarrow \ell \bar{\nu}_\ell X}$	$27.0 \pm 7.8$ (< 1%)
$N_{\Lambda_b^0 \text{ Other}'}$	$7.2 \pm 6.8$ (< 1%)
$N_{B \text{ Other}'}$	$3.5 \pm 0.3$
$N_{\Lambda_b^0 \rightarrow \Sigma_c^+ \pi^-}$	$0.763917 \pm 0.112236$
$N_{B \rightarrow \ell \bar{\nu}_\ell X}$	$0.643348 \pm 0.27741$
$N_{\Lambda_b^0 \rightarrow \Lambda_c^+ X}$	$0.097919 \pm 0.0217996$
$N_{\Lambda_b^0 \rightarrow \Lambda_c^+ p^-}$	$0.0265047 \pm 0.00408758$

TABLE III: Normalizations for all backgrounds in the  $\Lambda_b^0$  signal window  $m(\Lambda_c^+ \pi^-) \in [5.565, 5.670] \text{ GeV}/c^2$ . Only the first seven components are included in the lifetime fit.

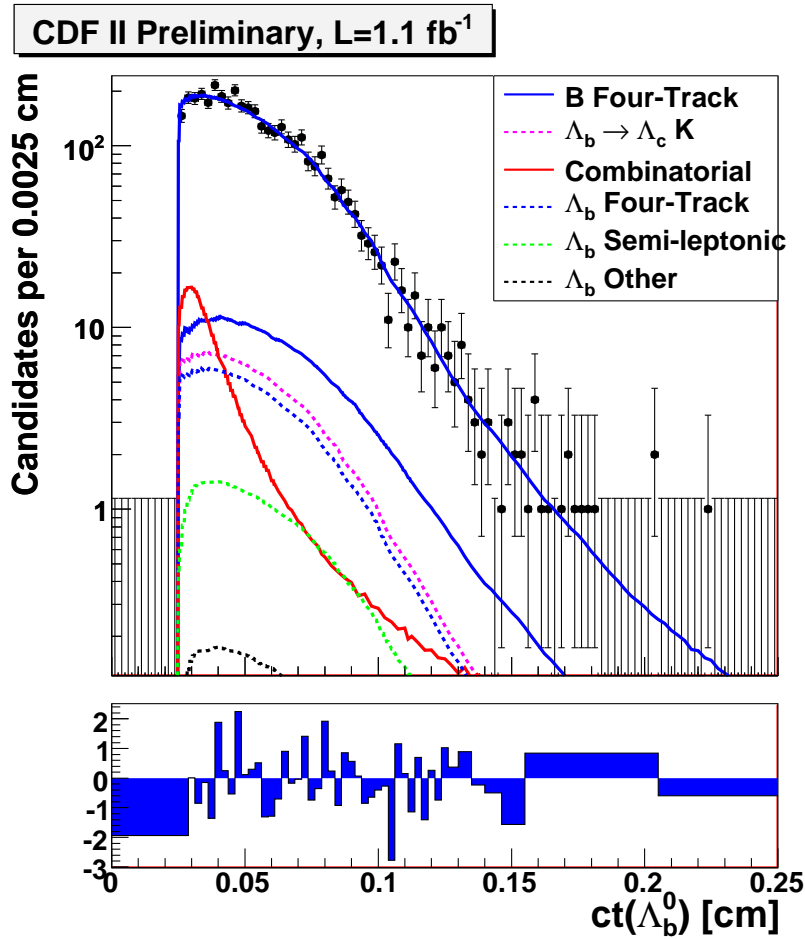


FIG. 6:  $\Lambda_b^0$  lifetime fit on data. The projection of the 3-dimensional likelihood of the fit for  $\tau(\Lambda_b^0)$  on the  $ct$  axis.

To gain confidence in the results various cross-checks have been performed. Figure 7 shows results of lifetime fits performed on Monte Carlo samples generated with  $\Lambda_b^0$  lifetimes,  $325\mu\text{m}$ ,  $368\mu\text{m}$  and  $500\mu\text{m}$ . The fitter returns correct result over a significant range of input lifetimes. We have used our fitter framework to measure  $B^0$  lifetime in the  $B^0 \rightarrow D^{*-} \pi^+$  decay mode, which is in agreement with the world average. We have confirmed that the  $\Lambda_b^0$  lifetime result doesn't change appreciably due to moving up the lower edge of the mass window by  $15 \text{ MeV}/c^2$  or by splitting the signal region into two halves. Finally we have split the data into 3 significant data taking periods and have found them compatible within statistical errors.

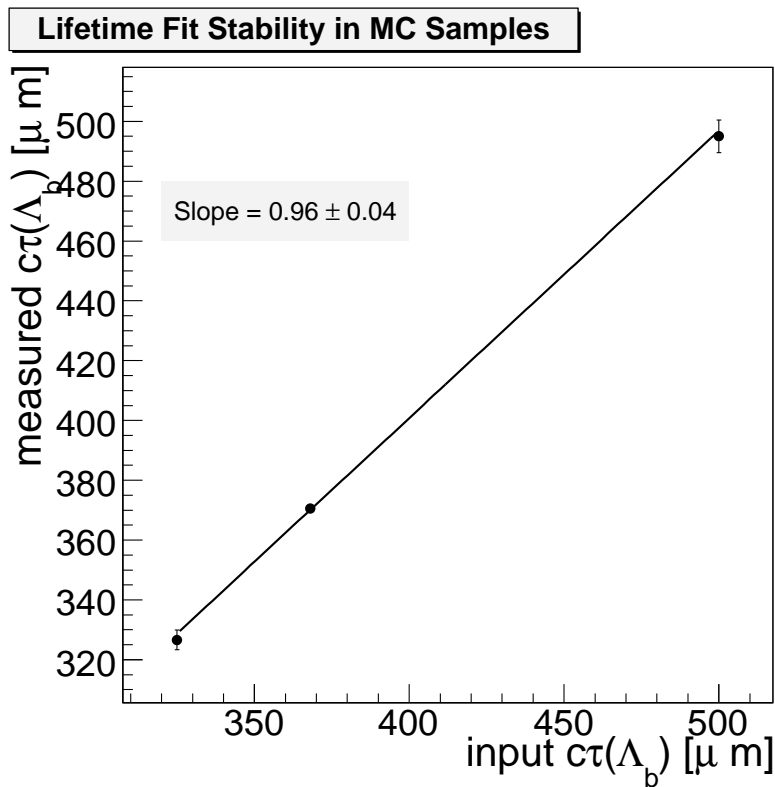


FIG. 7:  $\Lambda_b^0$  lifetime fit results from Monte Carlo samples generated with  $325\mu\text{m}$ ,  $368\mu\text{m}$  and  $500\mu\text{m}$  lifetimes.

### A. Systematics

According to their effect on calculating the SVT efficiency, we consider two broad groups of systematic errors: those that bias the SVT efficiency, and those that do not. Most of the sources of systematic error fall in the latter category and are evaluated using a modified Toy Monte Carlo technique. For the parameters associated with an individual systematic, we generate Toy Monte Carlo samples where these parameters are varied. The sample is fit with both the default fit and the fit with varied parameters. We take the difference between the values of  $\Lambda_b^0$  lifetime in the ‘varied’ (a.k.a. ‘rigged’) fit and the ‘default’ fit. This difference, caused by the systematic variation, constitutes the associated systematic error. After generating and fitting 1000 Toy Monte Carlo samples, the resulting distribution is fit with a Gaussian, and the mean is taken as the systematic shift due to that particular systematic.

The sources of systematic uncertainty are listed in Table IV. The total systematic uncertainty is computed by adding all sources of systematic error in quadrature. Our total systematic error, thus obtained, is  $10.6\mu\text{m}$ . The leading sources of systematic error are due to lack of knowledge of the SVT modeling in Monte Carlo,  $\Lambda_c^+$  decay Dalitz structure and combinatorial  $ct$  template.

The systematic error due to deficiency in SVT trigger modeling as well as silicon hit simulation in Monte Carlo is evaluated using a  $J/\psi \rightarrow \mu\mu$  sample collected using the CDF di-muon trigger. Unlike the SVT triggered samples the  $J/\psi$  decay length distribution of this sample is not biased. We reconstruct  $J/\psi$ 's in this sample and calculate SVT efficiency as the ratio of  $J/\psi$  candidates passing the SVT cuts and the total number of  $J/\psi$  candidates in the sample in  $L_{xy}(J/\psi)$  bins. To ensure maximum compatibility between data and Monte Carlo events, we generate fake events with the 3-momenta of the reconstructed data events and primary vertex positions. We pass them through CDF detector and SVT trigger simulations and calculate SVT efficiency the same way as in data. Figure 8 shows the ratio of data and MC SVT efficiencies fitted to a first order polynomial. We apply the resulting slope to the SVT efficiency as a multiplicative factor and evaluate the systematic error using the Toy Monte Carlo method described above.

Our baseline Monte Carlo is generated with the  $\Lambda_c^+$  Dalitz decay branching fractions set to the PDG [4] values. A comparison between data and Monte Carlo  $\Lambda_c^+$  Dalitz distributions suggest the MC modeling to be largely inadequate to reproduce data. The systematic error, due to the Dalitz fractions, is therefore estimated very conservatively. Several random ensembles are generated; the value of each fraction is fluctuated, between  $\pm 3\sigma$  of the PDG error, using a flat prior distribution. The systematic is computed using the usual Toy Monte Carlo method. The RMS of the resulting shifts from the baseline lifetime result is quoted as the systematic.

Description	Value [ $\mu\text{m}$ ]
Alignment	2.0
SVT-SVX d0 correlation	1.0
Background Normalizations	1.0
Mass Template Shapes	negligible
SVT Model	8.6
Data-MC Agreement: $\Lambda_c^+$ Dalitz structure	3.7
Combinatorial $ct$ Template	2.9
Data-MC Agreement: TrigCode re-weighting	2.0
Data-MC Agreement: $\Lambda_b^0$ polarization	1.4
Data-MC Agreement: Primary Vertex Position	1.2
$B^0$ Efficiency	1.0
$B^0$ Lifetime	1.0
Data-MC Agreement: $pt(\Lambda_b^0)$ spectrum	negligible
$\sigma_{ct}$ Scale Factor	negligible
Fitter Bias	negligible
$\sigma_{ct}$ Binning	negligible
$\Lambda_c^+$ Lifetime	negligible
Data-MC Agreement: Primary Vertex Error	negligible
Total Systematic Uncertainty	10.6

TABLE IV: Summary of the systematic uncertainties. The first group listed in the table are non-SVT-biased sources of systematic error. The total systematic uncertainty is obtained by adding the result of all systematics in quadrature.

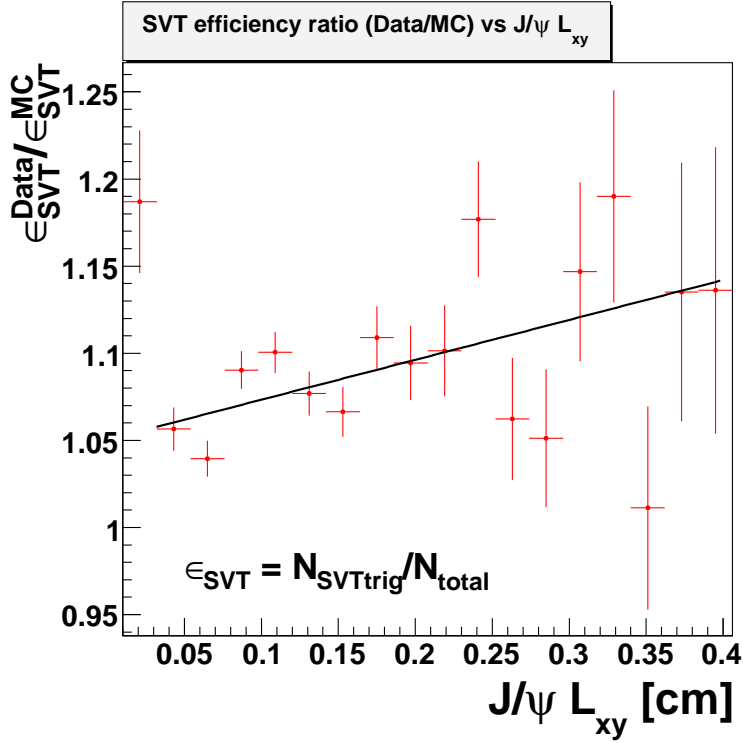


FIG. 8: Ratio of data and Monte Carlo SVT efficiencies fitted to a first order polynomial.

In the baseline fit the combinatorial background  $ct$  is modeled with a Landau distribution obtained by fitting candidates in the upper sideband of data. We obtain a rigged template by smoothing the same sideband candidate distribution rather than fitting it. The systematic error is obtained using our modified Toy Monte Carlo method as explained above.

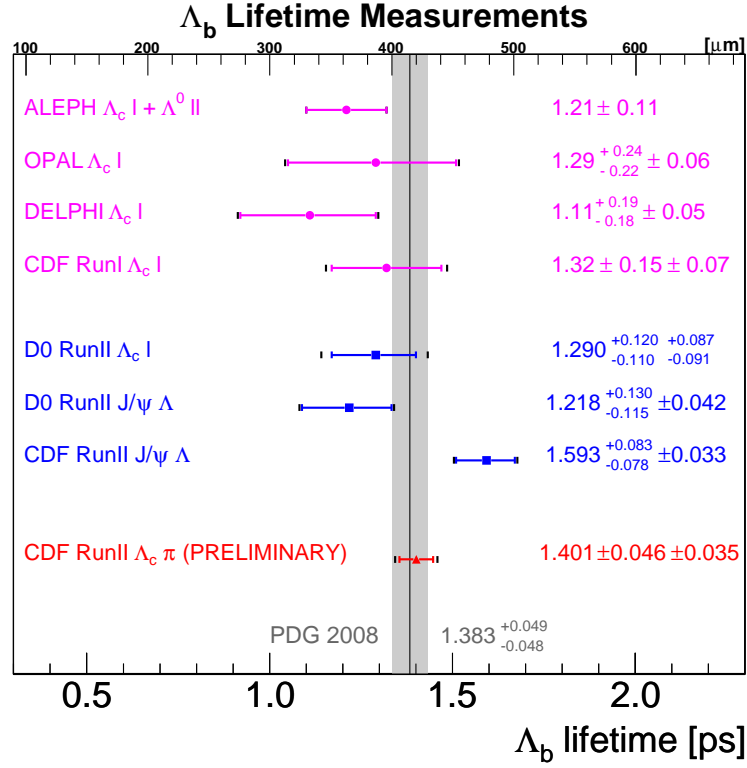


FIG. 9: Our  $\Lambda_b^0$  lifetime measurement is compared with the current world average (HFAG 2008) and all measurements contributing to it.

## V. SUMMARY

Analyzing a sample of  $\sim 3000$  fully reconstructed  $\Lambda_b^0 \rightarrow \Lambda_c^+ \pi^-$  decays from  $1070 \pm 60 \text{ pb}^{-1}$  of data, collected with two displaced track triggers, we measure the lifetime of the  $\Lambda_b^0$  baryon to be:

$$c\tau(\Lambda_b^0) = 420.1 \pm 13.7 \text{ (stat)} \pm 10.6 \text{ (syst)} \mu\text{m}.$$

It is expressed in picoseconds as:

$$\tau(\Lambda_b^0) = 1.401 \pm 0.046 \text{ (stat)} \pm 0.035 \text{ (syst)} \text{ ps}.$$

Using the current world average for  $B_d^0$  lifetime [7] we obtain:

$$\tau(\Lambda_b^0)/\tau(B^0) = 0.916 \pm 0.038.$$

In Figure 9 our result is compared with the current world average [8] for  $\Lambda_b^0$  lifetime. It is currently world's single most precise measurement. Shown also are all the measurements that contribute to the world average, including the last CDF measurement in the  $\Lambda_b^0 \rightarrow J/\psi \Lambda$  mode. We see an excellent agreement between our result and the current world average, which is dominated by the CDF  $\Lambda_b^0 \rightarrow J/\psi \Lambda$  result. Also, our result lies at the upper end of the the current HQE prediction [3] of  $\tau(\Lambda_b^0)/\tau(B^0) = 0.88 \pm 0.05$ , and prefers its most probable value of 0.94. This measurement thus resolves the puzzle concerning the long standing disagreement between the  $\Lambda_b^0$  lifetime ratio and its HQE prediction.

## Acknowledgments

We thank the Fermilab staff and the technical staffs of the participating institutions for their vital contributions. This work was supported by the U.S. Department of Energy and National Science Foundation; the Italian Istituto Nazionale di Fisica Nucleare; the Ministry of Education, Culture, Sports, Science and Technology of Japan; the Natural Sciences and Engineering

Research Council of Canada; the National Science Council of the Republic of China; the Swiss National Science Foundation; the A.P. Sloan Foundation; the Bundesministerium für Bildung und Forschung, Germany; the Korean Science and Engineering Foundation and the Korean Research Foundation; the Particle Physics and Astronomy Research Council and the Royal Society, UK; the Institut National de Physique Nucleaire et Physique des Particules/CNRS; the Russian Foundation for Basic Research; the Comisión Interministerial de Ciencia y Tecnología, Spain; and in part by the European Community's Human Potential Programme under contract HPRN-CT-20002, Probe for New Physics.

---

- [1] I. I. Y. Bigi, M. A. Schifman and N. Uraltsev, *Ann.Rev.Nucl.Part.Sci.* **47** (1997) 591.
- [2] N. Uraltsev, *Phys. Lett.* B376 (1996) 303.  
D. Pirjol and N. Uraltsev, *Phys. Rev.* D59 (1999) 034012.  
P. Colangelo and F. De Fazio, *Phys. Lett.* B387 (1996) 371.  
M. Di Pierro, C. Sachrajda, C. Michael, *Phys. Lett.* B468 (1999) 143.
- [3] C. Tarantino *et al.*, arXiv:hep-ph/**0310241**
- [4] W. M. Yao *et al.*, *J. Phys. G* **33**, 1(2006).
- [5] A. Abulencia, *et al.* (hep-ex/0609021)
- [6] The CDF Collaboration, CDF public note 9203.
- [7] W. M. Yao *et al.*, *J. Phys. G* **33**, 1(2006) and 2007 partial update for the 2008 edition.
- [8] Heavy Flavor Averaging Group's 2008 compilation of  $B$  lifetimes. <http://www.slac.stanford.edu/xorg/hfag/>